

# Oral Selumetinib Does Not Negatively Impact Photoreceptor Survival in Murine Experimental Retinal Detachment

Colleen M. Cebulla,<sup>1</sup> Bongsu Kim,<sup>1</sup> Valerie George,<sup>1</sup> Tyler Heisler-Taylor,<sup>1,2</sup> Sumaya Hamadmad,<sup>1</sup> Alana Y. Reese,<sup>1</sup> Shaili S. Kothari,<sup>1</sup> Rania Kusibati,<sup>1</sup> Hailey Wilson,<sup>1</sup> and Mohamed H. Abdel-Rahman<sup>1,3</sup>

<sup>1</sup>Havener Eye Institute, Department of Ophthalmology and Visual Science, The Ohio State University Wexner Medical Center, Columbus, Ohio, United States

<sup>2</sup>Department of Biomedical Engineering, The Ohio State University College of Engineering, Columbus, Ohio, United States

<sup>3</sup>Division of Human Genetics, Department of Internal Medicine, The Ohio State University Wexner Medical Center, Columbus, Ohio, United States

Correspondence: Colleen M. Cebulla, Havener Eye Institute, The Ohio State University, 915 Olentangy River Road, Suite 5000, Columbus, OH 43212, USA; colleen.cebulla@osumc.edu.

Submitted: August 9, 2018

Accepted: November 26, 2018

Citation: Cebulla CM, Kim B, George V, et al. Oral selumetinib does not negatively impact photoreceptor survival in murine experimental retinal detachment. *Invest Ophthalmol Vis Sci.* 2019;60:349–357. <https://doi.org/10.1167/iovs.18-25405>

**PURPOSE.** Mitogen-activated protein kinase/extracellular signal-regulated kinase (MAPK/ERK) signaling is neuroprotective in some retinal damage models but its role in neuronal survival during retinal detachment (RD) is unclear. In addition, serous RDs are a prevalent side effect of MEK inhibitors (MEKi), blocking MAPK/ERK signaling for treatment of certain cancers. We tested the hypothesis that MEKi treatment in experimental RD would increase photoreceptor death.

**METHODS.** The MEKi selumetinib was delivered daily to C57BL/6 mice at a clinically relevant dose (10 mg/mL) starting 1 day prior to creating RD with subretinal hyaluronic acid injection. Photoreceptor TUNEL and outer nuclear layer (ONL) thickness were analyzed. Phospho-ERK1/2 (pERK) distribution, glial fibrillary acidic protein (GFAP) accumulation, and Iba-1 (microglia/macrophages) were evaluated with immunofluorescence.

**RESULTS.** pERK accumulated in the Müller glia in detached retinas, but this was effectively blocked by selumetinib. Selumetinib did not induce serous RDs at day 1 and did not increase TUNEL positive photoreceptors or further decrease ONL thickness compared to controls. Retinal gliosis was not altered, but selumetinib did block the increase in intraretinal microglia/macrophage Iba-1 fluorescence intensity and acquisition of amoeboid morphology.

**CONCLUSIONS.** MAPK/ERK is neuroprotective in some retinal damage models; in RD, selumetinib blocked Müller pERK accumulation and changed the retinal microglia/macrophage phenotype but did not alter photoreceptor survival. This is consistent with the relatively good visual acuity seen in patients developing transient retinal detachments on MEK inhibitor therapy. Compensation by other neuroprotective pathways in the retina during retinal detachment may occur in the presence of MEK inhibition.

**Keywords:** selumetinib (AZD6244), MAPK/ERK pathway, retinal detachment, Müller glia, MEK inhibitor

Retinal detachment (RD) is a major cause of visual impairment. Types of RD include (1) rhegmatogenous, from a retinal break, (2) tractional, from fibrous proliferation as in diabetic retinopathy or proliferative vitreoretinopathy (PVR), or (3) serous/exudative, the category that does not lead to PVR, which results from abnormal leakage in the subretinal space.<sup>1</sup> Rhegmatogenous RD is common, and standard surgical treatment for RD cannot always prevent permanent visual loss, as RD leads to a variety of destructive mechanisms including photoreceptor apoptosis, retinal gliosis and fibrosis, retinal ischemia, and inflammation.<sup>2</sup> A large research effort seeks to understand these mechanisms and the natural systems that the retina has in place to protect itself from damage, in which the Müller glia appear to take a central role.

According to growing evidence, Müller glia appear to be responsible for the neuroprotection of the retina in many

experimental models of retinal damage. Many of the endogenous protective responses rely on the stimulation of survival signal transduction pathways. The mitogen-activated protein kinase/extracellular signal-regulated kinase (MAPK/ERK) pathway is a kinase cascade that mediates a variety of cell functions, including proliferation, differentiation, survival, apoptosis, and stress response.<sup>3</sup> Activation of the MAPK/ERK cascade has been demonstrated in the Müller glia in experimental models of retinal damage, including experimental retinal detachment.<sup>4–6</sup> In other models of retinal damage, the activation of MAPK/ERK in Müller glia has been shown to generate Müller glia that are neuroprotective of photoreceptors.<sup>7–10</sup> While involvement of the MAPK/ERK pathway in experimental RD has been established in proliferation responses of Müller glia,<sup>4–6</sup> any neuroprotective potential has not been evaluated.

Our recent work showed that inhibiting the proinflammatory cytokine macrophage migration inhibitory factor (MIF) was neuroprotective in experimental RD and that this protection was accompanied by an interesting increase in pERK accumulation in the Müller glia.<sup>11</sup> We theorized that stimulation of the MAPK/ERK pathway in Müller glia has indirect neuroprotective functions for the photoreceptors in RD, as it does for other models of retinal damage. Moreover, the function of the MAPK/ERK pathway in the retina has become an increasingly important question with the advent of MEK inhibitors used clinically to treat several malignancies. Interestingly, serous retinal detachment is a side effect of this class of drug.<sup>12-14</sup> If activation of the MAPK/ERK pathway is an endogenous neuroprotective mechanism during retinal detachment, could patients taking these medications be at risk of more permanent vision loss?

We hypothesized that inhibiting the MAPK/ERK pathway with selumetinib (AZD6244)—a drug used in clinical trials of targeted therapy for multiple malignancies<sup>15</sup>—would negate this protective mechanism during experimental RD and increase apoptosis. To investigate this, we developed an oral method of delivering selumetinib to mice with experimental RD using a dose that corresponds to therapeutic dosing in patients.<sup>16</sup> We observed the activation of MAPK/ERK, as indicated by the accumulation of pERK in the detached retina. Despite the importance of MAPK/ERK signaling in several animal models, oral selumetinib blocked retinal pERK accumulation during RD but did not increase photoreceptor toxicity, nor did it induce serous RDs after 1 day of treatment.

## METHODS

### Fabrication of Selumetinib (AZD6244) Jelly Pellets

Selumetinib, also known as AZD6244 (10 mg/kg, S1008; Selleck Chemicals, Houston, TX, USA) is a MAPK/ERK inhibitor at the level of MEK. We prepared it in a strawberry jelly pellet (100  $\mu$ l) in a modification of a previously described protocol.<sup>17</sup> This method avoids stress and complications associated with oral gavage. The jelly was composed of 16% Splenda, 9.6% gelatin powder, 7.9% imitation strawberry flavoring extract, and 0.8% vehicle (DMSO) with or without AZD6244 (0.22 mg/jelly pellet for 22 g weight mouse). The solution was homogenized with DI water at room temperature without foaming. We used a multichannel pipette to place 100  $\mu$ l of solution onto paraffin film dimples casted on a 1000  $\mu$ l micropipette tip rack (Fig. 1). The casts of jellies were cured in the 4°C refrigerator for 15 minutes. The jelly pellets were gently peeled off from the paraffin film cast and stored at 4°C, protected from light, and consumed within 9 days of fabrication.

### Animals and Retinal Detachment Surgery

This research adheres to the principles of the ARVO Statement for the Use of Animals in Ophthalmic and Vision Research. It was conducted under a protocol approved by The Ohio State University Institutional Animal Care and Use Committee. The mice were housed in ALAC-approved facilities at The Ohio State University. The mice were kept on a cycle of 12 hours light starting at 6 AM, followed by 12 hours dark. Groups of five mice were housed in standard Nalgene cages and received water and food ad libitum.

Retinal detachments (RD) were induced by subretinal injection of approximately 5  $\mu$ l undiluted hyaluronic acid (HA, 10 mg/ml, AMO) into left eyes of 22- to 24-week-old

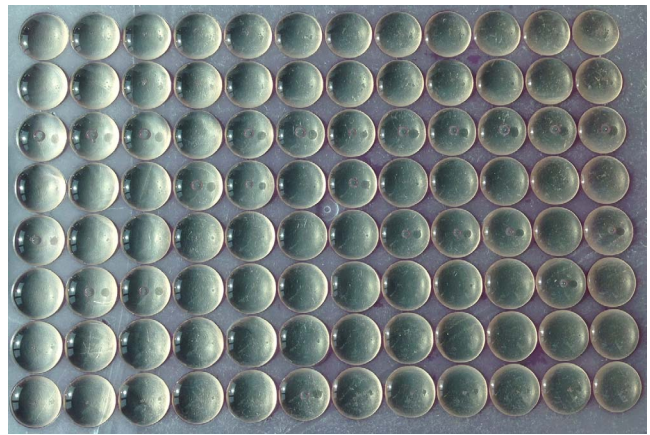


**FIGURE 1.** Selumetinib (AZD6244) jelly pellet fabrication. Identical shape and volume (100  $\mu$ l) of strawberry flavored selumetinib jelly pellets were fabricated on the engraved parafilm sheet cast on a 1000  $\mu$ l micropipette tip rack.

female C57BL/6 mice as previously described.<sup>18</sup> Untreated right eyes served as controls.

### Selumetinib (AZD6244) Oral Delivery Training and Study Design

**Oral Training.** To train the mice to consume the jelly tablets, animals were single caged with water and a jelly pellet without vehicle or selumetinib for approximately 1 hour, then returned to their original cages. Training was successful over a 3-day period and consumption was typically completed within 15 minutes.

**Experimental Design.** After training, the mice ( $n = 6-8$ /group) were given either vehicle or selumetinib infused jelly pellets (0.22 mg AZD6244 pellet; 10 mg/kg for a standard 22 g mouse) once per day starting on experimental day  $-1$ . Retinal detachments were induced on day 0. Mice were euthanized on day 3, 7, or 14. Mice were excluded from analysis if there was a large hemorrhage ( $n = 2$ ).

### Enucleation and Fixation

Mice were euthanized and eyes enucleated. A small opening was cut in the temporal limbus to allow better penetration of fixative. The eye was placed in fixative containing phosphate buffer with 4% paraformaldehyde and 30% sucrose in 0.1 M phosphate buffer at pH 7.4 for 30 minutes. Eyes were washed twice in PBS for 10 minutes and placed in 30% sucrose in PBS overnight at 4°C. The eyes were embedded in optimal cutting temperature (OCT) solution (Electron Microscopy Sciences, Hatfield, PA, USA), then snap frozen and cut into 12 micron sections.

### Immunohistochemistry (IHC)

Immunofluorescence staining was performed to detect markers as previously described<sup>19</sup> using antibodies to SOX2 (Y-17, goat polyclonal IgG; Santa Cruz Biotechnology, Inc., Dallas, TX, USA) or glial fibrillary acidic protein (GFAP; G3893, mouse monoclonal IgG1; Sigma-Aldrich Corp., St. Louis, MO, USA) and pERK1/2 (4370S, rabbit mAb; Cell Signaling Technology, Danvers, MA, USA) and Iba-1 (catalog #016-20001, rabbit anti-Iba-1; Wako Chemicals, Richmond, VA, USA). Slides were blocked with PBS containing 5% bovine serum albumin, and 1% Triton X-100. Alexa Fluor 488 or 568 conjugated secondary antibodies were used (1:1000; Invitrogen/Thermo Fisher,

Fremont, CA, USA) after 30-minute incubation with 100% normal donkey serum. Omission of the primary antibody was used as a control for background staining; omission of primary and secondary antibodies was used as a control for autofluorescence. Cell nuclei were counterstained with DAPI (Invitrogen) and DRAQ5 (4084; Cell Signaling).

### TUNEL Assay

The TUNEL assay (In Situ Cell Death Kit, TMR red, 1215679910; Roche Applied Science, Pleasanton, CA, USA) was performed as per the manufacturer's instructions on frozen sections as previously described.<sup>19</sup> Slides were washed by antibody diluent then 1× PBS. TMR red kit was applied for 1 hour in the humidified chamber at 37°C. After washing by 1× PBS, DAPI was applied to stain the nuclei.

### Image Analysis

Photomicrographs were obtained using a Leica DM5000B fluorescent microscope and Leica DC500 digital camera. Confocal images were obtained using a Leica SP8 imaging system at the Hunt-Curtis Department of Neuroscience Imaging Facility. To minimize the variability of region-specific differences within the retina, the same region of retina was evaluated for the fellow-eye control and retinal detachment areas. Identical illumination, microscope, and camera settings were used. Fixed areas were randomly sampled across all retinal layers in areas of detachment and in similar control retina areas. The retina was selected as the region of interest from the 20× field of view for both fluorescent and confocal microscopy and analyzed in a masked fashion. Counts, mean area, and intensity density were determined with ImageJ (1.48v; <http://imagej.nih.gov/ij/>; provided in the public domain by the National Institutes of Health, Bethesda, MD, USA) in threshold designated regions. TUNEL analysis was performed using a custom ImageJ macro as described.<sup>20</sup> The ONL thicknesses were determined with ImageJ by measuring the ONL thickness to total retinal thickness ratios in 5 areas on each image (500–750 micron width) with 3 to 5 images per animal. Intraretinal microglia/macrophage morphology from immunofluorescence images were evaluated in a masked fashion with a 1–3 grading scale by 3 reviewers (Supplementary Fig. S1): 1 = predominantly spindle (<20% amoeboid), 2 = mixed (20–35% amoeboid), 3 = predominantly amoeboid (>35% amoeboid). Confocal images were analyzed as Max Intensity Projections of Z-Stack image captures. Image color intensities were optimized for ImageJ-based thresholding and cell selection using a modified version of our previously established ImageJ macro.<sup>20</sup> In addition, Iba-1 confocal images were analyzed using a form factor 1 analysis ( $FF1 = 4\pi^2 \text{Area} / [\text{perimeter}]^2$ )<sup>21</sup> to assess the cell morphology. Figure images were optimized for color, brightness, and contrast using GIMP 2.8; double-labeled images were overlaid using LAS X (Version 2.0.0.14332) or ImageJ.

### Statistical Analysis

Two-tailed unpaired Student's *t*-test was performed to confirm a difference in measurements with two independent groups with continuous data. One-tailed testing was used for the maximal FF1 comparison in which prior experiments demonstrated a one-directional decrease after treatment. Error bars show SEM. For retinal microglia/macrophage grading analysis, the likelihood ratio test was performed in JMP (version 11; SAS Institute, Cary, NC, USA) through ordinal contingency analysis. JMP and Microsoft Excel (Professional Plus 2010) were used for statistical analysis.  $P \leq 0.05$  was considered significant.

## RESULTS

### ERK1/2 Phosphorylation in Retinal Detachment

To determine if the MAPK/ERK cascade was activated in Müller glia in our mouse model of retinal detachment, dual immunostaining of Müller glial markers (SOX2 and GFAP) and pERK was performed at day 3 ( $n = 6$ ) and 7 ( $n = 5/\text{group}$ ) post detachment. pERK accumulated in detached retinas in comparison to control (Fig. 2). Furthermore, pERK immunofluorescence colocalized in the nuclei and cytoplasm of Sox2 positive cells, indicating that the MAPK/ERK cascade was highly activated in Müller glia. Consistent with the findings of Geller et al.<sup>4</sup> in experimental RD, pERK in control retinas was visualized at low levels in the Müller glial endfeet and presumably astrocytes in the ganglion cell layer (GCL). In RD, we found pERK increased significantly in detached retina at day 7 and had a trend toward significance at day 3 compared to control retina ( $P = 0.0025$  day 7 and  $P = 0.0960$  day 3); pERK accumulation was observed in Müller glia endfeet in the GCL and was very abundant in the inner nuclear layer (INL), colocalizing with Sox2 in the Müller glia nuclei with weaker levels in the cytoplasm. Similarly, Kase et al.<sup>5</sup> detected pERK accumulation in the nuclei of the INL in their mouse model of retinal detachment.

Geller et al.<sup>4</sup> found in their rabbit and cat models that pERK accumulated in the retinal pigment epithelia (RPE) rapidly after RD but to a lesser degree and with lesser duration than that of Müller glia. RPE cells did not stain significantly for pERK in our mouse model of RD (not shown). It is possible that the RPE cells have pERK accumulation at an earlier timepoint than those tested in this study. Furthermore, it could be that our mouse model does not parallel the findings of the rabbit and cat models, as Kase et al.<sup>5</sup> similarly did not detect pERK accumulation in RPE in their mouse model of RD.

### Oral Selumetinib (AZD6244) Blocks Retinal pERK Accumulation

To investigate if oral delivery of selumetinib successfully inhibited the MAPK/ERK cascade by preventing the phosphorylation of ERK in Müller glia, we compared pERK immunofluorescence in selumetinib or vehicle-treated eyes with retinal detachments. On day 3, selumetinib-treated eyes, in comparison with vehicle-treated eyes, experienced a significant 1.85 fold reduction ( $P = 0.0040$ ) in the mean intensity of pERK immunofluorescence of the inner nuclear layer (INL) ( $89.406 \pm 11.954$  mean intensity/mm<sup>2</sup> retina selumetinib versus  $165.450 \pm 26.525$  mean intensity/mm<sup>2</sup> retina vehicle). Similarly, at day 7, there was a significant 1.79 fold reduction ( $P = 0.0050$ ) in mean intensity of pERK of the INL in the selumetinib-treated eyes in comparison with vehicle-treated eyes ( $95.548 \pm 12.843$  mean intensity/mm<sup>2</sup> retina selumetinib versus  $171.202 \pm 14.941$  mean intensity/mm<sup>2</sup> retina vehicle). The reduction of pERK indicates that oral delivery of selumetinib was successful in inhibiting the retinal MAPK/ERK cascade during retinal detachment.

### Oral Selumetinib Does Not Block Photoreceptor Apoptosis in Retinal Detachment

To investigate the effect of selumetinib on photoreceptor apoptosis, the TUNEL assay was performed on selumetinib- and vehicle-treated eyes with retinal detachments. Selumetinib treatment of RD did not significantly increase ( $P = 0.5192$ ) TUNEL positive cells in the ONL compared to vehicle treatment ( $1138.687 \pm 637.071$  cells/mm<sup>2</sup> retina selumetinib versus  $1691.024 \pm 526.842$  cells/mm<sup>2</sup> retina vehicle; Fig. 3).

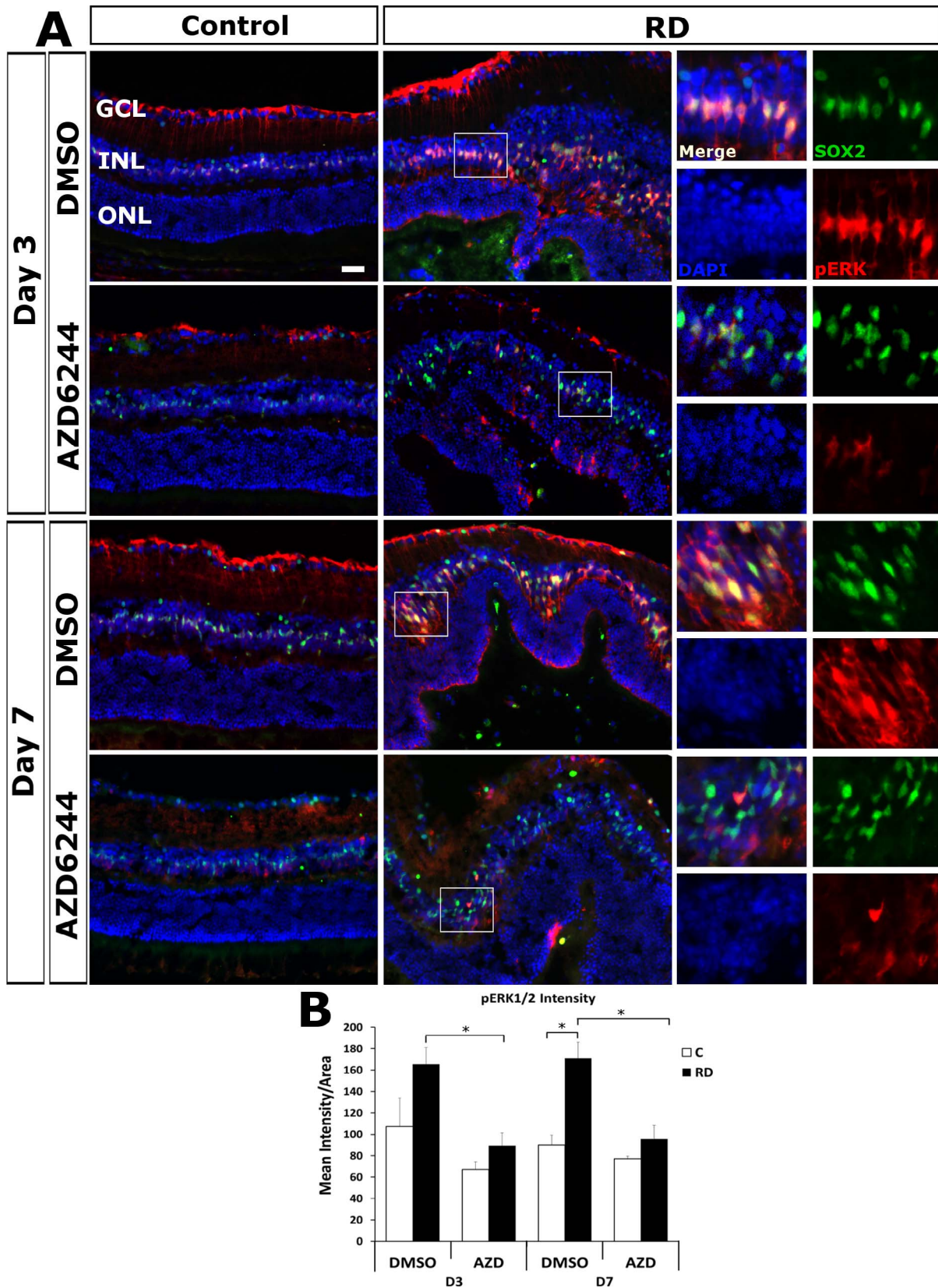


**FIGURE 2.** Selumetinib (AZD6244) blocks the increased accumulation of Müller pERK in RD. **(A)** Representative images of immunofluorescence for pERK1/2 (red) and Müller marker Sox2 (green) with DAPI counterstain for nuclei (blue) for day 3 ( $n = 6$  mice/group) and day 7 ( $n = 5$  mice/group) RD and fellow eye controls. pERK accumulates in the detached Müller endfeet in the GCL. The insert areas to the right highlight the colocalization of pERK1/2 and Sox2 accumulation in the INL; pERK was significantly increased after RD compared to control ( $P = 0.0960$  day 3;  $P = 0.0025$  day 7). pERK1/2 accumulation was blocked in Müller glia in RD eyes of selumetinib treated mice at day 3 ( $P = 0.0040$ ) and day 7 ( $P = 0.0050$ ) compared to vehicle treated eyes. Scale bar denotes 50 microns. **(B)** Quantitation of retinal pERK1/2 intensity  $*P < 0.05$ .

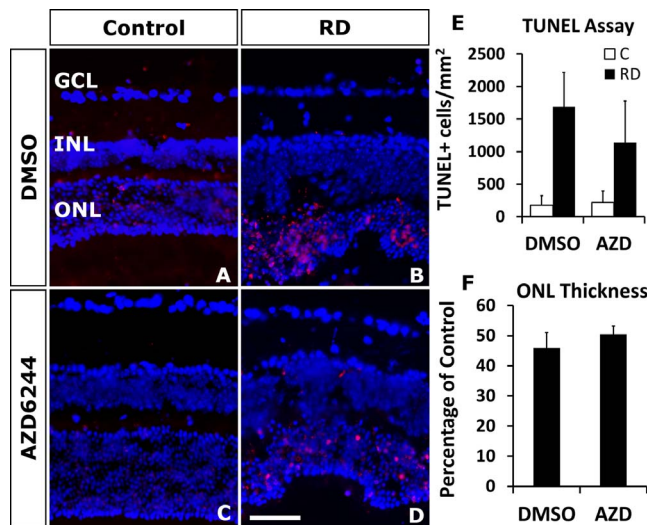


**FIGURE 3.** Selumetinib (AZD6244) does not increase cell death in detached photoreceptors. Representative day 3 RD images with TUNEL positive cells (red) counterstained with DAPI (blue) (A–D). There was no significant increase in TUNEL positive photoreceptors in RD eyes treated with selumetinib (D) compared to vehicle (B). Quantitation (E) showed no difference ( $P = 0.5192$ ,  $n = 6$  mice/group). (F) There was no difference in the ONL thickness ratio at day 14 between the selumetinib and vehicle treated RD groups ( $P = 0.450$ ,  $n = 8$  mice/group). Scale bar denotes 50 microns.

To further investigate the effect of selumetinib treatment on photoreceptor apoptosis, we determined the ratio of ONL thickness to retinal thickness. The resulting ONL thickness percentage at day 14 post RD was not significantly different between vehicle- and selumetinib-treated groups ( $P = 0.450$ ), with both groups decreasing to approximately 50% of control ONL thickness.

### Oral Selumetinib Does Not Alter Müller Expression of GFAP

The upregulation of intermediate filaments, namely GFAP and vimentin, is a prominent feature of the experimental RD damage response. Nakazawa et al.<sup>6</sup> demonstrate that genetic depletion of the dual intermediate filaments in mice was neuroprotective in experimental RD. Furthermore, these genetically depleted mice experienced diminished ERK phosphorylation in response to retinal detachment. Similarly, a number of other retinal damage models have detected that the upregulation of intermediate filaments in Müller glia is parallel to the activation of the MAPK/ERK cascade.<sup>4,9,22</sup> Despite this potential significance for photoreceptor neuroprotection, little is known regarding the role of the MAPK/ERK pathway in regulation of GFAP expression following retinal damage. In models of brain damage, pERK accumulation colocalized with GFAP upregulation in astrocytes and MEK inhibitors diminished GFAP expression and neuronal apoptosis.<sup>23,24</sup> Since the connection between the upregulation of these intermediate filaments and MAPK/ERK in the retina remains unclear, we investigated if MEK inhibition comparably altered GFAP expression in Müller glia by immunostaining for GFAP. Day 14 retinal detachment eyes all experienced an increase in GFAP, regardless of selumetinib or vehicle treatment. Although there was a trend toward lower expression, selumetinib treatment of RD retina was not significantly different ( $P = 0.0881$ ) in GFAP expression in comparison to vehicle treatment ( $170.142 \pm 18.487$  cells/mm<sup>2</sup> retina selumetinib versus  $232.264 \pm 27.896$  cells/mm<sup>2</sup> retina vehicle; Fig. 4).

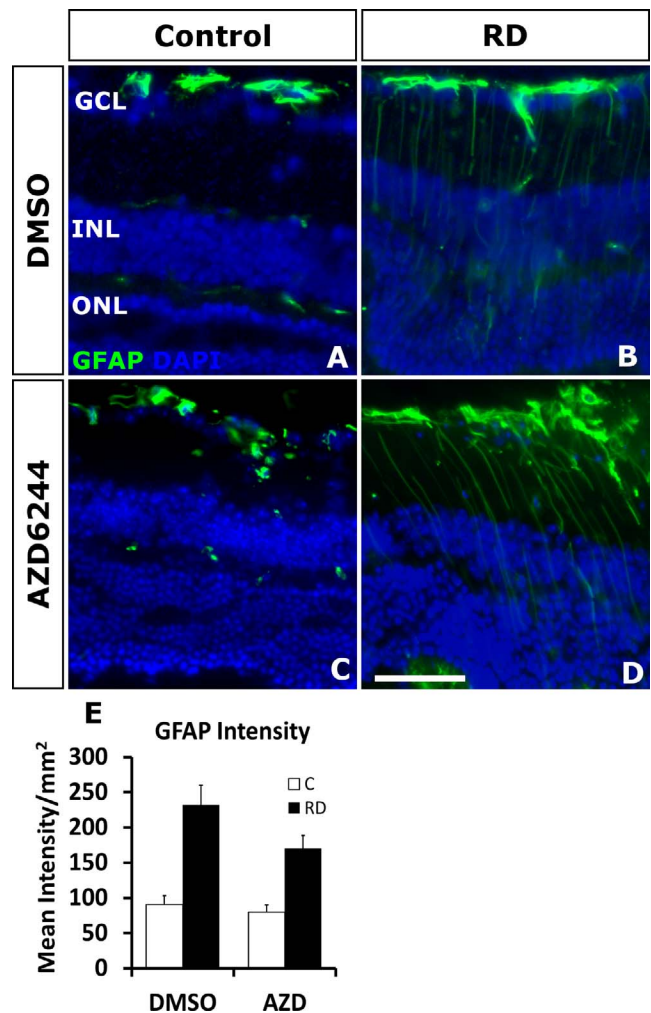


**FIGURE 4.** Oral selumetinib (AZD6244) does not significantly impact increased GFAP accumulation in RD. Immunofluorescence staining shows GFAP accumulation (green) after RD (B, D) compared with attached controls (A, C) at day 7 ( $n = 6$ /group). (E) Treatment with selumetinib does not significantly reduce GFAP staining in detached retina ( $P = 0.881$ ). Scale bar denotes 50 microns.

These results suggest that ERK phosphorylation is not necessary for the induction of GFAP during RD.

### Microglia Phenotype Is Altered by Selumetinib in Experimental RD

Microglia, the resident tissue macrophages of the retina, and infiltrating macrophages can have both neuroprotective and neurotoxic effects during retinal damage and play a critical role in damage processes.<sup>25–28</sup> To investigate the effects of selumetinib on microglial response during experimental RD, intraretinal Iba-1 intensity and microglial/macrophage morphology were assessed at day 14. There was an expected significant accumulation of Iba-1 intensity in detached retina compared to fellow eye controls ( $254.14 \pm 13.282$  intensity/mm<sup>2</sup> retina RD versus  $198.93 \pm 16.606$  intensity/mm<sup>2</sup> retina control,  $P = 0.02217$ ; Fig. 5E). Interestingly, the administration of selumetinib, compared to vehicle, significantly decreased microglia Iba-1 intensity in detached retina ( $212.75 \pm 10.78$  intensity/mm<sup>2</sup> retina selumetinib versus  $254.14 \pm 13.282$  intensity/mm<sup>2</sup> retina vehicle;  $P = 0.0306$ ). Retinal Iba-1+ cell counts were decreased in the selumetinib RD group compared

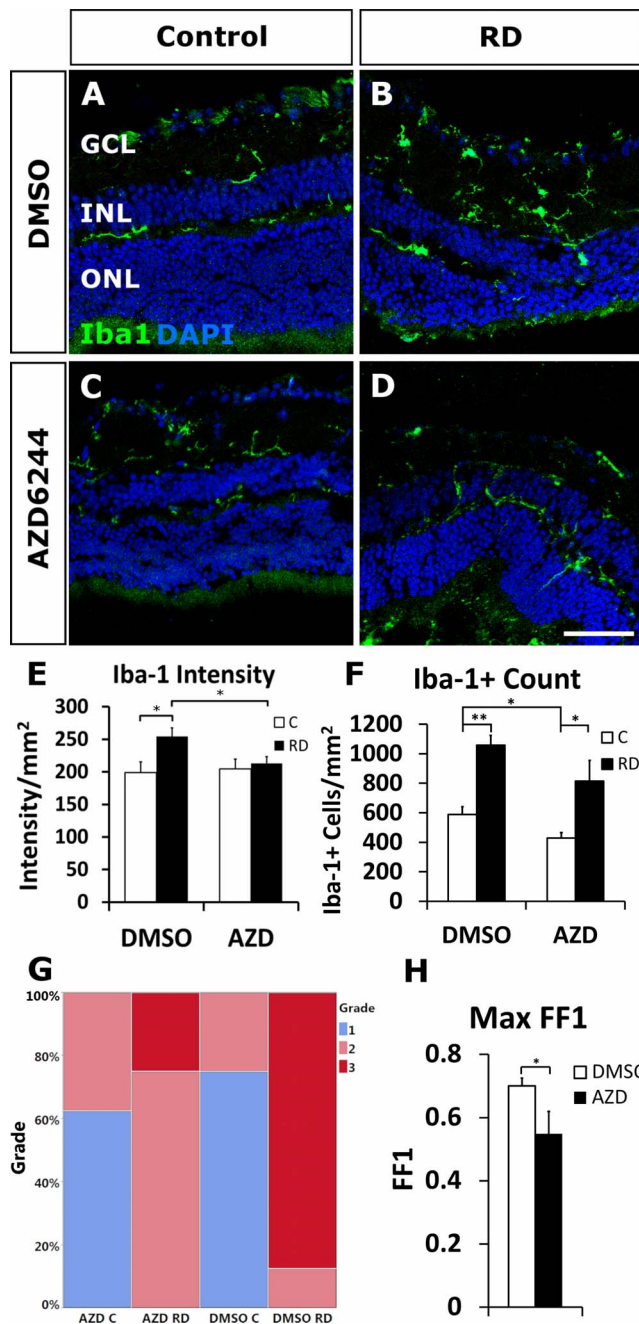


**FIGURE 5.** Oral selumetinib (AZD6244) reduces Iba-1 intensity and amoeboid morphology of microglia RD. Confocal images of immunofluorescent staining for Iba-1 (green) in microglia/macrophages shows more amoeboid morphology in vehicle treated RD versus control mice (A, B). Selumetinib treatment (C, D) resulted in less amoeboid and more tamified microglia/macrophage morphology in RD compared with vehicle treatment (B). The intensity of fluorescence signal was measured resulting in a significant increase in vehicle treated RD eyes compared to control ( $P = 0.0222$ ; E) and a significant decrease in AZD-treated RD eyes compared to vehicle-treated RD eyes ( $P = 0.0306$ ; E). Iba-1 positive cell counts per  $\text{mm}^2$  were significantly increased in RD eyes compared to controls in both selumetinib- and vehicle-treated eyes ( $P = 0.0291$  and  $P = 0.00009$ , respectively; F) and higher in vehicle compared with selumetinib treated controls ( $P = 0.0276$ ; F). Contingency table of microglia morphologic grade (G) showed a significant increase in amoeboid morphology (grade 3) in vehicle treated RD compared to selumetinib treated RD ( $P = 0.0086$ ). Cell morphology was also determined using the form factor 1 (FF1) value, resulting in a significant decrease of amoeboid cells in selumetinib treated eyes ( $P = 0.0357$ ; H). Scale bar denotes 50 microns.

with the vehicle RDs, but this did not reach statistical significance ( $813.85 \pm 140.19$  cells/ $\text{mm}^2$  selumetinib RD versus  $1057.58 \pm 65.99$  cells/ $\text{mm}^2$  control RD;  $P = 0.1469$ ; Fig. 5F). The increase in Iba-1+ counts in RD versus fellow eye control remained significant in both the vehicle and selumetinib groups ( $P = 0.00009$  and  $P = 0.02914$ , respectively; Fig. 5F). Importantly, intraretinal microglial/macrophage morphology in RD was significantly different in selumetinib-treated animals compared to vehicle-treatment animals, based upon the phenotype grading scale and maximal form factor 1 values (likelihood test,  $P = 0.0086$  and one-tailed  $t$ -test,  $P = 0.03572$ , respectively; Figs. 5G, 5H). The selumetinib RD group had a more spindle-shaped phenotype with 75% grade 2 (Fig. 5G; contingency table), compared to the vehicle RD group, which appeared more amoeboid shaped—typical of an activated morphology—with 90% grade 3 scores. These results are confirmed by the form factor 1 analysis at the maximal values as higher values represent cells of a more amoeboid morphology. Together, the results suggest that selumetinib impacts the intraretinal microglia/macrophage phenotype in the detached retina.

### DISCUSSION

Activation of the MAPK pathway has been known to have a pro-oncogenic effect, resulting in increased cellular proliferation and tumor cell survival.<sup>29</sup> The development of targeted cancer therapeutics with MEK inhibitors is promising for the treatment of many cancers. However, these treatments have notable ocular toxicities, particularly the development of self-limited serous RDs in up to 90% of patients.<sup>12</sup> These MEK inhibitor-induced RDs are defined by bilateral subretinal fluid foci with a normal choroid and normal retinal pigment epithelium (RPE), making them morphologically unique.<sup>12</sup> More importantly, these detachments do not typically induce irreversible loss of vision.<sup>14,12</sup> Our findings concur with these data, as inhibition of the MAPK/ERK pathway with oral selumetinib did not elicit additional damage to detached photoreceptors in our rhegmatogenous RD experimental murine model, correlating to the generally reversible visual changes in MEK inhibitor-treated patients.

For this study, we modified a protocol by El-Hoss et al.<sup>17</sup> to deliver selumetinib orally in the form of a strawberry-flavored jelly. El-Hoss prepared the drug delivery jelly in culture plates and cut it into doses for delivery to the mouse model. We modified the protocol to create pellets of consistently equal shape and volume during production, as described in the Methods section. Oral delivery of selumetinib more accurately represents patient absorption and metabolism of selumetinib than previous intravenous methods in mice models, and this method avoids potential complications and stress associated with oral gavage techniques.<sup>17</sup> Importantly, this method effectively blocked pERK accumulation in the retina. Thus, oral delivery has the potential to be extended into an in vivo model aimed at studying these side effects in the retina.

We did not visualize any selumetinib-induced serous RDs or retinal abnormalities in the mice after 1 day of treatment at the time of RD creation with subretinal Healon injection. It is unclear whether our lack of pERK staining in the RPE in this mouse model (similar to that of Kase et al.<sup>5</sup>) could be one factor in the lack of serous RD development in this model. Other factors include drug dosage/timing, species, and lack of a more sensitive detection method, such as spectral domain optical coherence tomography (SD-OCT). Parameters could be explored in the future to facilitate developing an alternative animal model to study the mechanism behind this ocular side effect and factors regulating subretinal fluid.

This study evaluated the impact of MAPK/ERK inhibition in a murine experimental RD model, particularly since the neuroprotective role of this pathway had not been formally explored. The model is considered a good model for rhegmatogenous RD in which liquefied vitreous enters a retinal break and detaches the retina. The subretinal injection of hyaluronic acid (HA) is relevant since HA is the major component of vitreous. In contrast, the type of RD induced by MEK inhibitor therapy is serous/exudative, with accumulation of fluid under the retina. An animal model of serous RD would be useful since there is still relatively little known about the mechanism of MEK inhibitor-induced RDs. Jiang et al.<sup>30</sup> determined that aquaporin 1 channels (AQP1) within the RPE are regulated in part by the MAPK/ERK pathway. Administration of MEK inhibitors PD98059 and U0126 blocked the down-regulation of AQP1 that occurs in response to UV and oxidative stress.<sup>30</sup> Decreased AQP1 expression on the RPE could lead to a reduction in fluid pumping from the subretinal space and be a potential mechanism of subretinal fluid accumulation and serous retinal detachment seen in patients taking MEK inhibitors.<sup>30,31</sup> The AQP1 hypothesis should be evaluated in future studies if an animal model of MEK inhibitor-related serous RD can be developed. In addition, in patients, the serous RD may resolve after temporary withdrawal of the MEK inhibitor. Reintroduction of the medication is not always associated with re-detachment. This may suggest a potential feedback loop in which receptor responses or levels that maintain the retinal homeostasis are altered. It would be interesting to explore this finding in the future with development of an animal model.

This study evaluated the impact of MEK/ERK inhibition on photoreceptor survival after a relatively short duration of treatment to study impacts on photoreceptor damage in experimental RD at standard key timepoints for the model. However, it did not evaluate the effects of long-term MEK inhibitor treatment on photoreceptor responses. Future studies with longer-term evaluations could be considered. In addition, studies with electrophysiology to directly evaluate retinal function would be very valuable. The current study used surrogate markers of retinal function.

In Müller glia, stimulation of the MAPK/ERK cascade has been demonstrated in many experimental models of retinal damage, including diabetic retinopathy,<sup>9</sup> NMDA-induced injury,<sup>8</sup> bright-light exposure,<sup>10,32</sup> inflammatory stimulation,<sup>22</sup> retinal stretch,<sup>33</sup> and, as confirmed in our results, experimental retinal detachment.<sup>4-6</sup> Various chemical signals are known to also be responsible for the initiation of the MAPK/ERK cascade in Müller glia, including but not limited to heparin-binding epidermal-like growth factor (HG-EGF),<sup>34</sup> fibroblastic growth factor (FGF2)<sup>35,36</sup> and nerve growth factor (NGF),<sup>37</sup> brain-derived neurotrophic factor (BDNF),<sup>36</sup> and ciliary neurotrophic factor (CNTF).<sup>36</sup>

Previous reports have established that the MAPK/ERK cascade is involved in generating proliferative, migratory, progenitor-like, and neuroprotective Müller glia in retinal damage.<sup>8-10,35</sup> The impact of MAPK/ERK on retinal neuroprotection was evaluated in some of these damage models. For example, in the N-methyl-D-aspartate (NMDA) in vivo retinal injury model Nakazawa et al.<sup>8</sup> showed that ERK1<sup>-/-</sup> mice lacked the upregulation of pERK1/2 after NMDA intravitreal injection and had upregulation of TUNEL-positive inner retinal neurons greater than twofold compared to controls. Similarly, Fischer et al.<sup>35</sup> showed in the NMDA chick model that FGF2 selectively induced pERK in Müller glia and that pretreatment with FGF2 before NMDA would induce significant neuroprotection of inner retinal neurons, although the impact of MEK inhibitors on cell death was not specifically evaluated in that model. In an in vivo axotomized rat model, BDNF intravitreal

injection at the time of axotomy caused a burst of MAPK and AKT activation at 1 hour that was sustained over 3 days. Intravitreal pretreatment with MEK/ERK inhibitor U0126 showed a greater effect than inhibitor PD98059 and partially blocked the neuroprotective effect of intravitreally injected BDNF on axotomized RGCs.<sup>38</sup> Interestingly, the PI3 kinase-inhibitor LY294002 also partially blocked cell death. In contrast to these studies that found inhibition of neuroprotection with U0126, in the rat light damage model, upregulation of pERK was detected in the GCL, and intraocular U0126 reduced retinal pERK as well as activated caspase-3 expression on the western blot.<sup>39</sup> The article did not directly evaluate the impact of TUNEL/activated caspase immunofluorescence and cell loss after U0126 treatment.<sup>40</sup>

Ex vivo and in vitro studies have also evaluated the impact of MEK/ERK inhibition on retinal cell survival during damage. In a murine retinal explant model, treatment with MEK inhibitor U0126 significantly increased TUNEL positive cells in a culture, particularly in the GCL and INL at 24 and 48 hours.<sup>10</sup> In an in vitro high glucose damage model of primary rat retinal cultures, mixed glial/neuronal retinal cultures were protected from dying when compared with pure neuronal cultures; blocking pERK with PD98059 increased apoptosis in the mixed glial/neuronal cultures.<sup>9</sup> MEK inhibition was found to block the neuroprotective effects of exogenous placental growth factor in two in vitro damage models in cell lines RGC-5 (oxygen-glucose deprivation) and 661W (light-induced cell death).<sup>41</sup> In contrast, in a light-induced injury model of 661W cells, pretreatment with MEK inhibitor PD98059 significantly suppressed light-induced autophagy and protected 661W cells from 3 days of light injury.<sup>42</sup>

Our results demonstrate that the MAPK/ERK pathway did not have measurable neuroprotective effects on photoreceptors in this experimental RD model. It is possible that in the context of rhegmatogenous experimental (hyaluronic acid injection-induced) RD treated with MEK inhibitor, the neuroprotective pathways that are activated by MAPK/ERK are compensated by other pathways. In RD, activation of at least STAT3, CREB, and NF- $\kappa$ B has been noted in addition to MAPK/ERK.<sup>4</sup> There exists some evidence of interactions between MAPK/ERK and these pathways in various tissues,<sup>43-45</sup> but the extent of cross-talk between these pathways in the retina is yet uncertain. Future studies will be needed to explore these interactions. In addition, the impact of MAPK/ERK1/2 can have differential functions depending on cell type, duration of activation, and the association with other mediators.<sup>46</sup>

Microglial cells in the CNS play an important role in immune response, maintenance of neural circuitry, and tissue homeostasis.<sup>47</sup> We found that inhibiting the MAPK/ERK pathway with selumetinib in experimental RD blocked the increase in Iba1 intensity and acquisition of the amoeboid morphology, typical of activated microglial cells.<sup>48</sup> Our findings that inhibition of MAPK/ERK may alter microglia activation are consistent with those in other experimental models of retinal damage. In a streptozocin diabetic rat model, Ibrahim et al.<sup>49</sup> found accumulation of activated, amoeboid microglia strongly positive for Iba1 in diabetic compared to non-diabetic retinas. Inhibition of the MAPK pathway in this model using a MEKi (U0126), but not JNK inhibitor (SP610025) blocked TNF- $\alpha$  release from microglia in response to Amadori-glycated albumin.<sup>49</sup> Similarly, in a peripheral nerve neuropathic pain model, Calvo et al.<sup>50</sup> showed that MEKi (U0126), delivered intrathecally, prevented microgliosis, amoeboid microglia morphology, and mechanical and cold pain hypersensitivity, which were seen in the control in response to neuregulin-1 injection. Previous studies have demonstrated that sustained microglial responses and products have contributed to neuronal and vascular cell death<sup>51</sup> and the progression of

retinal degeneration<sup>52</sup> and glaucoma.<sup>53</sup> However, critical neuroprotective effects of microglia in retinal damage have also been identified.<sup>26,27</sup> Okunuki et al.<sup>27</sup> discovered that activation of microglia in acute RD would inhibit photoreceptor cell death and play a role in injured photoreceptor removal. Further investigation into the role of MAPK/ERK signaling and impact on the microglia during retinal damage will be an interesting line of future research to dissect microglia-related damage mechanisms.

In conclusion, our results confirm previous cat, rabbit, and mouse models that the MAPK/ERK pathway is activated in Müller glia in a mouse model of experimental RD. Blocking the pathway with the clinically relevant MEKi selumetinib was neither neuroprotective nor neurotoxic for detached photoreceptors. These data correspond with the clinical finding of little loss of visual acuity in patients with serous retinal detachments form MEKi cancer therapy.

### Acknowledgments

Supported by NEI Award Number K08EY022672 and NCATS Award Number KL2TR001068. The content is solely the responsibility of the authors and does not necessarily represent the official views of the funding institutions. Additional funds were provided by the Ohio Lions Eye Research Foundation, OSU Fund #313310, and the Patti Blow Fund.

Disclosure: **C.M. Cebulla**, None; **B. Kim**, None; **V. George**, None; **T. Heisler-Taylor**, None; **S. Hamadmad**, None; **A.Y. Reese**, None; **S.S. Kothari**, None; **R. Kusibati**, None; **H. Wilson**, None; **M.H. Abdel-Rahman**, None

### References

- Jalali S. Retinal detachment. *Comm Eye Health*. 2003;16:25-26.
- Garweg JG, Tappeiner C, Halberstadt M. Pathophysiology of proliferative vitreoretinopathy in retinal detachment. *Surv Ophthalmol*. 2013;58:321-329.
- Wortzel I, Seger R. The ERK cascade: distinct functions within various subcellular organelles. *Genes Cancer*. 2011;2:195-209.
- Geller SF, Lewis GP, Fisher SK. FGFR1, signaling, and AP-1 expression after retinal detachment: reactive Müller and RPE cells. *Invest Ophthalmol Vis Sci*. 2001;42:1363-1369.
- Kase S, Yoshida K, Harada T, et al. Phosphorylation of extracellular signal-regulated kinase and p27(KIP1) after retinal detachment. *Graefes Arch Clin Exp Ophthalmol*. 2006;244:352-358.
- Nakazawa T, Takeda M, Lewis GP, et al. Attenuated glial reactions and photoreceptor degeneration after retinal detachment in mice deficient in glial fibrillary acidic protein and vimentin. *Invest Ophthalmol Vis Sci*. 2007;48:2760-2768.
- Akiyama H, Nakazawa T, Shimura M, Tomita H, Tamai M. Presence of mitogen-activated protein kinase in retinal Müller cells and its neuroprotective effect ischemia-reperfusion injury. *Neuroreport*. 2002;13:2103-2107.
- Nakazawa T, Shimura M, Ryu M, et al. ERK1 plays a critical protective role against N-methyl-D-aspartate-induced retinal injury. *J Neurosci Res*. 2008;86:136-144.
- Matteucci A, Gaddini L, Villa M, et al. Neuroprotection by rat Müller glia against high glucose-induced neurodegeneration through a mechanism involving ERK1/2 activation. *Exp Eye Res*. 2014;125:20-29.
- Groeger G, Doonan F, Cotter TG, Donovan M. Reactive oxygen species regulate prosurvival ERK1/2 signaling and bFGF expression in gliosis within the retina. *Invest Ophthalmol Vis Sci*. 2012;53:6645-6654.
- Kim B, Kusibati R, Heisler-Taylor T, et al. MIF inhibitor ISO-1 protects photoreceptors and reduces gliosis in experimental retinal detachment. *Sci Rep*. 2017;7:14336.
- Francis JH, Habib LA, Abramson DH, et al. Clinical and morphologic characteristics of MEK inhibitor-associated retinopathy. *Ophthalmology*. 2017;124:1788-1798.
- Sheyman AT, Scarinci F, Fawzi AA, Gill MK. Long-term evaluation of MEK inhibitor retinal toxicity with multimodal imaging. *Ophthalmic Surg Lasers Imaging Retina*. 2016;47:76-77.
- Urner-Bloch U, Urner M, Stieger P, et al. Transient MEK inhibitor-associated retinopathy in metastatic melanoma. *Ann Oncol*. 2014;25:1437-1441.
- Ciombor KK, Bekaii-Saab T. Selumetinib for the treatment of cancer. *Expert Opin Investig Drugs*. 2015;24:111-123.
- Denton CL, Gustafson DL. Pharmacokinetics and pharmacodynamics of AZD6244 (ARRY142886) in tumor-bearing nude mice. *Cancer Chemother Pharmacol*. 2011;67:349-360.
- El-Hoss J, Kolind M, Jackson MT, et al. Modulation of endochondral ossification by MEK inhibitors PD0325901 and AZD6244 (selumetinib). *Bone*. 2014;59:151-161.
- Cebulla CM, Ruggeri M, Murray TG, Feuer WJ, Hernandez E. Spectral domain optical coherence tomography in a murine retinal detachment model. *Exp Eye Res*. 2010;90:521-527.
- Cebulla CM, Zelinka CP, Scott MA, et al. A chick model of retinal detachment: cone rich and novel. *PLoS One*. 2012;7:12.
- Heisler-Taylor T, Kim B, Reese AY, et al. A new multichannel method quantitating TUNEL in detached photoreceptor nuclei. *Exp Eye Res*. 2018;176:121-129.
- Hepner FL, Roth K, Nitsch R, Hailer NP. Vitamin E induces ramification and downregulation of adhesion molecules in cultured microglial cells. *Glia*. 1998;22:180-188.
- Takeda M, Takamiya A, Yoshida A, Kiyama H. Extracellular signal-regulated kinase activation predominantly in Müller cells of retina with endotoxin-induced uveitis. *Invest Ophthalmol Vis Sci*. 2002;43:907-911.
- Li Y, Chen D, Li Y, et al. Oncogenic cAMP responsive element binding protein 1 is overexpressed upon loss of tumor suppressive miR-10b-5p and miR-363-3p in renal cancer. *Oncol Rep*. 2016;35:1967-1978.
- Zhang L, Zhao W, Li B, et al. TNF-alpha induced overexpression of GFAP is associated with MAPKs. *Neuroreport*. 2000;11:409-412.
- Nakazawa T, Hisatomi T, Nakazawa C, et al. Monocyte chemoattractant protein 1 mediates retinal detachment-induced photoreceptor apoptosis. *Proc Natl Acad Sci U S A*. 2007;104:2425-2430.
- Gallina D, Zelinka C, Fischer AJ. Glucocorticoid receptors in the retina, Müller glia and the formation of Müller glia-derived progenitors. *Development*. 2014;141:3340-3351.
- Okunuki Y, Mukai R, Pearsall EA, et al. Microglia inhibit photoreceptor cell death and regulate immune cell infiltration in response to retinal detachment. *Proc Natl Acad Sci U S A*. 2018;115:E6264-E6273.
- Nakazawa T, Kayama M, Ryu M, et al. Tumor necrosis factor-alpha mediates photoreceptor death in a rodent model of retinal detachment. *Invest Ophthalmol Vis Sci*. 2011;52:1384-1391.
- Grimaldi AM, Simeone E, Festino L, Vanella V, Strudel M, Ascierto PA. MEK Inhibitors in the treatment of metastatic melanoma and solid tumors. *Am J Clin Dermatol*. 2017;18:745-754.
- Jiang Q, Cao C, Lu S, et al. MEK/ERK pathway mediates UVB-induced AQP1 downregulation and water permeability impairment in human retinal pigment epithelial cells. *Int J Mol Med*. 2009;23:771-777.

31. Stamer WD, Bok D, Hu J, Jaffe GJ, McKay BS. Aquaporin-1 channels in human retinal pigment epithelium: role in transepithelial water movement. *Invest Ophthalmol Vis Sci.* 2003;44:2803-2808.
32. Liu C, Peng M, Laties AM, Wen R. Preconditioning with bright light evokes a protective response against light damage in the rat retina. *J Neurosci.* 1998;18:1337-1344.
33. Lindqvist N, Liu Q, Zajadacz J, Franze K, Reichenbach A. Retinal glial (Müller) cells: sensing and responding to tissue stretch. *Invest Ophthalmol Vis Sci.* 2010;51:1683-1690.
34. Wan J, Ramachandran R, Goldman D. HB-EGF is necessary and sufficient for Müller glia dedifferentiation and retina regeneration. *Dev Cell.* 2012;22:334-347.
35. Fischer AJ, Scott MA, Ritchey ER, Sherwood P. Mitogen-activated protein kinase-signaling regulates the ability of Müller glia to proliferate and protect retinal neurons against excitotoxicity. *Glia.* 2009;57:1538-1552.
36. Wahlström KJ, Campochiaro PA, Zack DJ, Adler R. Neurotrophic factors cause activation of intracellular signaling pathways in Müller cells and other cells of the inner retina, but not photoreceptors. *Invest Ophthalmol Vis Sci.* 2000;41:927-936.
37. Wang J, He C, Zhou T, Huang ZJ, Zhou LL, Liu XL. NGF increases VEGF expression and promotes cell proliferation via ERK1/2 and AKT signaling in Müller cells. *Mol Vis.* 2016;22:254-263.
38. Nakazawa T, Tamai M, Mori N. Brain-derived neurotrophic factor prevents axotomized retinal ganglion cell death through MAPK and PI3K signaling pathways. *Invest Ophthalmol Vis Sci.* 2002;43:3319-3326.
39. Yang XW, Chen H, Zhu MH, et al. Up-regulation of PKM2 relates to retinal ganglion cell apoptosis after light-induced retinal damage in adult rats. *Cell Mol Neurobiol.* 2015;35:1175-1186.
40. Kassen SC, Thummel R, Campochiaro LA, Harding MJ, Bennett NA, Hyde DR. CNTF induces photoreceptor neuroprotection and Müller glial cell proliferation through two different signaling pathways in the adult zebrafish retina. *Exp Eye Res.* 2009;88:1051-1064.
41. Inoue Y, Shimazawa M, Nakamura S, et al. Protective effects of placental growth factor on retinal neuronal cell damage. *J Neurosci Res.* 2014;92:329-337.
42. Zhang TZ, Fan B, Chen X, et al. Suppressing autophagy protects photoreceptor cells from light-induced injury. *Biochem Biophys Res Commun.* 2014;450:966-972.
43. Wan J, Zhao XF, Vojtek A, Goldman D. Retinal injury, growth factors, and cytokines converge on beta-catenin and pStat3 signaling to stimulate retina regeneration. *Cell Rep.* 2014;9:285-297.
44. Kao DD, Oldebeken SR, Rai A, et al. Tumor necrosis factor-alpha-mediated suppression of dual-specificity phosphatase 4: crosstalk between NFkappaB and MAPK regulates endothelial cell survival. *Mol Cell Biochem.* 2013;382:153-162.
45. Sun C, He M, Ko WK, Wong AO. Mechanisms for luteinizing hormone induction of growth hormone gene transcription in fish model: crosstalk of the cAMP/PKA pathway with MAPK- and PI3K-dependent cascades. *Mol Cell Endocrinol.* 2014;382:835-850.
46. Subramaniam S, Unsicker K. ERK and cell death: ERK1/2 in neuronal death. *FEBS J.* 2010;277:22-29.
47. Fernandes A, Miller-Fleming L, Pais TF. Microglia and inflammation: conspiracy, controversy or control? *Cell Mol Life Sci.* 2014;71:3969-3985.
48. Davis EJ, Foster TD, Thomas WE. Cellular-forms and functions of brain microglia. *Brain Res Bull.* 1994;34:73-78.
49. Ibrahim AS, El-Remessy AB, Matragoon S, et al. Retinal microglial activation and inflammation induced by amadori-glycated albumin in a rat model of diabetes. *Diabetes.* 2011;60:1122-1133.
50. Calvo M, Zhu N, Grist J, Ma ZZ, Loeb JA, Bennett DLH. Following nerve injury neuregulin-1 drives microglial proliferation and neuropathic pain via the MEK/ERK pathway. *Glia.* 2011;59:554-568.
51. Krady JK, Basu A, Allen CM, et al. Minocycline reduces proinflammatory cytokine expression, microglial activation, and caspase-3 activation in a rodent model of diabetic retinopathy. *Diabetes.* 2005;54:1559-1565.
52. Yang LP, Li Y, Zhu XA, Tso MOM. Minocycline delayed photoreceptor death in rds mice through iNOS-dependent mechanism. *Mol Vis.* 2007;13:1073-1082.
53. Bosco A, Inman DM, Steele MR, et al. Reduced retina microglial activation and improved optic nerve integrity with minocycline treatment in the DBA/2J mouse model of glaucoma. *Invest Ophthalmol Vis Sci.* 2008;49:1437-1446.